

Corrosion Behavior of Magnesium in Naturally Aerated Stagnant Seawater and 3.5% Sodium Chloride Solutions

El-Sayed M. Sherif

Center of Excellence for Research in Engineering Materials (CEREM), College of Engineering, King Saud University, P. O. Box 800, Al-Riyadh 11421, Saudi Arabia

*E-mail: esherif@ksu.edu.sa

Received: 20 February 2012 / *Accepted:* 12 March 2012 / *Published:* 1 May 2012

Magnesium (Mg) and its alloys have increased applications in industry. These applications are getting limited due to Mg corrosion, especially in chloride containing environments, because of its high negative potential. The objective of the present work thus was to report the corrosion of Mg in stagnant solutions of the naturally aerated Arabian Gulf seawater (AGS) and 3.5% NaCl. Weight-loss (WtL) after different exposure periods and scanning electron microscopy (SEM) with X-ray analyzer (EDX) investigations along with cyclic potentiodynamic polarization (CPP), potentiostatic current-time (PCT), and electrochemical impedance spectroscopy (EIS) measurements were employed to achieve this objective. WtL experiments indicated that Mg dissolves linearly and its corrosion rate decreases in AGS and NaCl solutions when its exposure time increases in the range from 120 h to 600 h. CPP, PCT, and EIS measurements confirmed the data obtained by WtL that the increase of exposure time decreases the uniform. This effect also increases the severity of Mg pitting corrosion. Results together showed clearly that AGS is more aggressive towards Mg surface than 3.5% NaCl solutions at the same condition.

Keywords: Arabia Gulf seawater; corrosion behavior; magnesium; sodium chloride solutions

1. INTRODUCTION

Magnesium (Mg) and its alloys are the lightest of all structural metallic materials. Because of their low densities, good damping, excellent heat dissipation, good mechanical and electrical properties, and good electro-magnetic shield, they have been extensively used in many applications [1-9]. Mg is widely used for manufacturing of mobile phones, laptop computers, cameras, and other electronic components. Historically, Mg was one of the main aerospace construction metals and was

used for German military aircraft as early as World War I and extensively for German aircraft in World War II [10].

Mg is very reactive metal because of which, its free element is not naturally found on earth, though once produced, it is coated in a thin layer of its oxide. The formation of this layer on the surface of Mg and its alloys does not provide full protection against corrosion, especially in chloride containing environments. This occurs as the Cl^- ions from the surrounding environment penetrate the oxide layer and reach the surface of Mg then react with the metal substrate. The high corrosion susceptibility is also expected as a result of the high active potential of Mg. The presence of impurities and second phases within Mg alloys can be considered as active cathodic sites, which accelerate the local galvanic corrosion of the alloy matrix [11]. The presence of impurities such as iron, copper and nickel in low amounts increases the corrosion resistant of the Mg alloy. These elements if present in high contents will act as active cathodes with small hydrogen overvoltage and result in dissolution of the Mg matrix [12-14]. This explains why the corrosion and corrosion protection of Mg in different aggressive electrolytes have been reported [15-19].

The objective of the current work is to compare between the effects of naturally aerated stagnant Arabian Gulf seawater (AGS) and 3.5% sodium chloride (3.5% NaCl) solutions on the corrosion of magnesium after its immersion for 1 hour and 6 days. The study was carried out using weight-loss immersion test for 600 hours along with SEM/EDX investigations and variety of electrochemical measurements such as polarization (CPP), current time (PCT) and electrochemical impedance spectroscopy. It is well known that AGS is a complex mixture of inorganic salts, dissolved gases, suspended solids, organic matter and organisms [20,21]. It has inorganic salts that include Na^+ , Mg^{2+} , K^+ , Ca^{2+} , and Sr^{2+} as well as very high concentrations of chloride (24090 mg/L), and sulfate (3384 mg/L) ions. AGS also has HCO_3^- , Br^- , and F^- , with total dissolved solids (TDS) of 43800 mg/L [21]. The presence of such high TDS concentration represents a very corrosive medium. Oxygen content also has a marked effect on corrosivity of seawater. At the same time, 3.5% NaCl solution has been also reported to simulate the percentage of chloride ion in the seawater and to be an aggressive medium towards many metals and alloys [22-41].

2. EXPERIMENTAL PROCEDURE

AGS solution was brought directly from the Arabian Gulf at the eastern region of Saudi Arabia and sodium chloride (NaCl, Merck, 99%) were used as received. An electrochemical cell with a three-electrode configuration was used; a square magnesium electrode (circa 99% purity Mg having 1.2 cm side length and total surface of 1.44 cm^2), a platinum foil, and an Ag/AgCl electrode (in the saturated KCl) were used as the working, counter, and reference electrodes, respectively. The Mg rod for electrochemical measurements was prepared by welding a copper wire to a drilled hole was made on one face of the rod; the rod with the attached wire were then cold mounted in resin and left to dry in air for 24 h at room temperature.

Before measurements, the other face of the Mg electrode, which was not drilled, was polished successively with metallographic emery paper of increasing fineness up to 1200 grit. The electrode

was then cleaned using doubly-distilled water, degreased with acetone, washed using doubly-distilled water again and finally dried with a stream of dry air. In order to prevent the possibility of crevice corrosion during measurement, the interface between sample and resin was coated with Bostik Quickset, a polyacrylate resin.

The weight loss experiments were carried out using rectangular magnesium coupons having the same purity of magnesium rods with the dimension of 4.0 cm length, 2.0 cm width, and 0.4 cm thickness and the exposed total area of 54.0 cm². The coupons were polished and dried as for the case of Mg rods, weighted (initial weight, m_{int}), and then suspended in 300 cm³ AGS and 3.5% NaCl solutions for different exposure periods and up to 600 hours. After the designated exposure to the test solution, the coupons were rinsed with distilled water, dried between two tissue papers, and weighted again (final weight, m_{fin}). Weight-loss measurements were made in triplicate and the loss of weight was calculated by taking an average of these values. The maximum standard deviation in the observed weight loss was calculated to be $\pm 1.5\%$. The weight loss (Δm , mg.cm⁻²) and the corrosion rate (K_{Corr} , mg.cm⁻².h⁻¹) over the exposure period were calculated according to the previous studies as follows [40-43]:

$$\Delta m = \frac{m_{\text{int}} - m_{\text{fin}}}{A} \quad (1)$$

$$K_{\text{Corr}} = \frac{m_{\text{int}} - m_{\text{fin}}}{A t} \quad (2)$$

Where, m_{int} is the initial weight before immersion, m_{fin} is the final weight after exposure to the test solution, A is the total surface area, 54.0 cm², and t is the time of exposure in hours.

The SEM investigation and EDX analysis were obtained for the surface of magnesium specimens after their immersions in the test solution after 600 h exposure. The SEM images were collected by using a JEOL model JSM-6610LV (Japanese made) scanning electron microscope with an energy dispersive X-ray analyzer attached.

Electrochemical experiments were performed by using an Autolab Potentiostat (PGSTAT20 computer controlled) operated by the general purpose electrochemical software (GPES) version 4.9. The cyclic potentiodynamic polarization (CPP) curves were obtained by scanning the potential in the forward direction from -2000 to -800 mV against Ag/AgCl at a scan rate of 3.0mV/s; the potential was then reversed in the backward direction at the same scan rate. Potentiostatic current-time (PCT) experiments were carried out by stepping the potential of the magnesium electrodes at -1200 mV versus Ag/AgCl.

Electrochemical impedance spectroscopy (EIS) data were performed at corrosion potentials (E_{Corr}) over a frequency range of 100 kHz – 100 mHz, with an ac wave of ± 5 mV peak-to-peak overlaid on a dc bias potential, and the impedance data were collected using Powersine software at a rate of 10 points per decade change in frequency. All the electrochemical experiments were recorded for the Mg electrodes after 60 minutes and 6 days immersions in the test electrolytes before measurements. All measurements were also carried out at room temperature in freely aerated solutions.

3. RESULTS AND DISCUSSION

3.1. Weight-loss measurements and SEM / EDX investigations

Fig. 1 depicts the change of weight loss (Δm , mg cm^{-2} , calculated using Eq. (1)) as a function of immersion time for Mg coupons in 300 cm^3 of AGS and 3.5% NaCl solutions. It is clearly seen from Fig. 1 that the value of Δm for Mg in AGS and NaCl solutions increased linearly with increasing immersion time. This is due to the continuous dissolution of Mg under the aggressiveness action of AGS and NaCl solutions against Mg surface. It has been reported that [44] the anodic dissolution of Mg occurs due to its high reactivity up on the immersion of Mg in the test solution as follows;



Mg also forms an oxide layer, which is included in the anodic reaction according to the following reaction;



On the other hand, the cathodic reaction for Mg at these conditions is the hydrogen evolution because of the electron consumption on Mg occurs by the unloading of hydrogen ions as shown in Eq. (5) [45]. The hydrogen ions are produced due to the dissociated water represented by Eq. (6).



This produced hydroxide ions will react with the dissolved Mg cations resulted from Eq. (3), Mg^{2+} , to form magnesium hydroxide as follows;



The equilibrium between the water from the solution and its ions is disturbed and the reaction becomes stronger in one direction [45] as can be seen by the following reaction;



Although Mg forms MgO and $\text{Mg}(\text{OH})_2$ on its surface, its dissolution rapidly increases with increasing the exposure time. This is due to the fact that these forms are not compact and not protective and allow the aggressive ions from AGS and NaCl solutions to attack the Mg surface. It is also seen that the values of Δm for Mg in AGS solutions are higher than that obtained for Mg in NaCl ones. This proves that AGS is more corrosive than 3.5% NaCl solutions towards Mg surface.

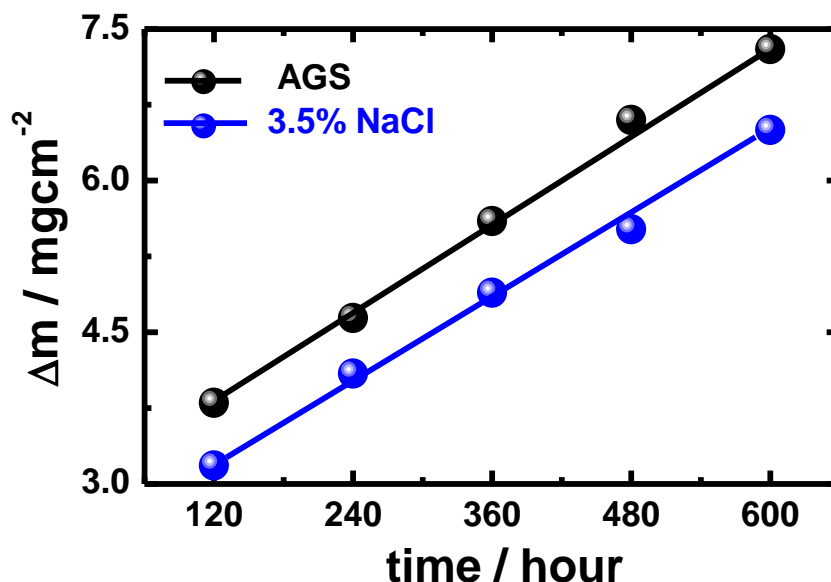


Figure 1. The variation of the weight-loss ($\Delta m / \text{mgcm}^{-2}$) as a function of time for Mg coupons in aerated AGS and 3.5% NaCl solutions.

The scanning electron microscope (SEM) images were taken for Mg surface after its immersion for 600 h in AGS and the micrographs are shown at different magnifications in Fig. 2a and Fig. 2b. The corresponding energy dispersive X-ray analyzer (EDX) profiles are respectively shown in Fig. 2c and Fig. 2d. The SEM micrograph, Fig. 2a, shows that the surface of Mg at this condition is completely covered with thick layer of corrosion products and there are few shaped like mushroom formed on the surface. The atomic percentages of the elements found in the mushroom like area of the SEM and displayed in the EDX profile presented in Fig. 2c, were 62.12% O, 16.11% C, 19.06% Ca, 0.14% Sr, and only 2.58% Mg. The small amounts of Mg indicate that the investigated mushroom like corrosion product is very thick and the compounds in this area might have formed on the Mg surface due to the presence of micro-organisms in the seawater.

Increasing the magnification of the SEM image in the flat area of the surface as shown in Fig. 2b, indicates that the surface composes of two regions; one is covered with grass like corrosion products from which the mushrooms were formed; and the other area is covered with a thin layer of corrosion products. The corresponding EDX profile analysis for the selected area of the SEM shown in Fig. 2b is shown in Fig. 2d. The atomic percentages of elements found in this area were, 66.70% O, 26.84% Mg, 3.99% C, 2.32% Ca, and 0.15% S. The high Mg content compared to that one found in the mushroom like area confirms that the thickness of corrosion products of the surface was smaller. The SEM/EDX investigations were also carried out for Mg surface after its immersion in 3.5% NaCl solutions for 600 h, where SEM micrographs of (a) a large area of the surface and (b) an extended area, which mainly contains white deposits, are respectively depicted by Fig. 3. The corresponding EDX profile analyses for the selected areas on the SEM images (a) and (b) are also shown in Fig. 3c and Fig. 3d, respectively. It is clearly seen from the SEM images that there are black and white areas. The atomic percentage of the elements found in the selected black area shown in Fig. 3a and represented by

the EDX profile shown in Fig. 3d, were 55.74% O, 41.76% Mg, 2.40% C, and 0.11% Mn. The elements found on the Mg surface suggest that the compounds formed at this condition were mainly magnesium oxide. On the other hand, the atomic percentages of the elements found in the white area of SEM image shown in Fig. 3b and displayed in the EDX profile presented in Fig. 3d, were 65.86% O, 30.14% Mg, and 4.00% C. this means that the oxide film in the white areas are more dense than the black areas as the percentage of O is higher.

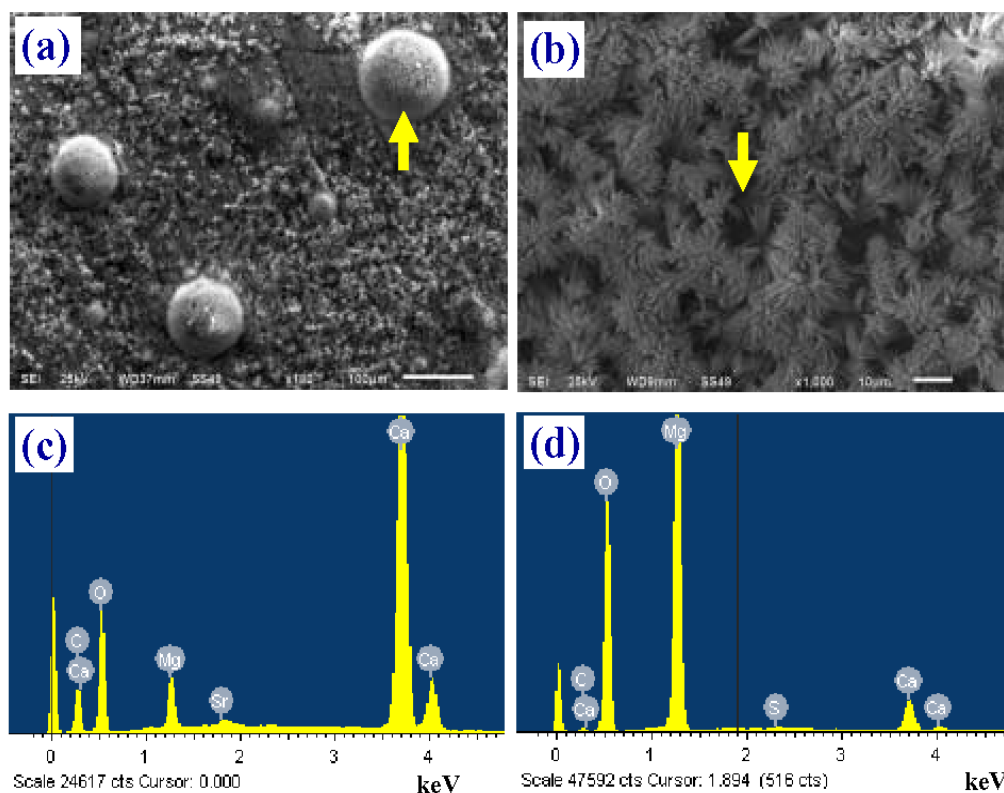


Figure 2. SEM micrographs (a) and (b) at different magnifications for magnesium surface after its immersion in naturally aerated AGS for 600 h; EDX profile analyses (c) and (d) taken in the selected SEM areas in image (a) and (b), respectively.

The values of K_{Corr} , which were calculated from weight-loss tests using Eq. (2) for Mg in AGS and 3.5% NaCl solutions, are plotted against time as shown in Fig. 4. The K_{Corr} of Mg recorded decreased values with increasing the immersion time in both AGS and NaCl solutions. The values of K_{Corr} for Mg in AGS were higher than those in 3.5% NaCl solutions at all the exposure periods. This proves that AGS is more corrosive towards Mg than 3.5% NaCl solutions at the same condition. Although, the SEM micrographs for Mg in AGS showed thick layer of corrosion products, the oxide film was more favorable to be formed on Mg in NaCl solutions, which may explain the higher values of Δm and K_{Corr} for Mg in AGS than those recorded in NaCl solutions. It is worth to mention also that the decrease of K_{Corr} for Mg in both media with decreasing the immersion time is due to the accumulation of corrosion products including magnesium oxide and hydroxide, which cover up the surface leading to decrease its uniform corrosion.

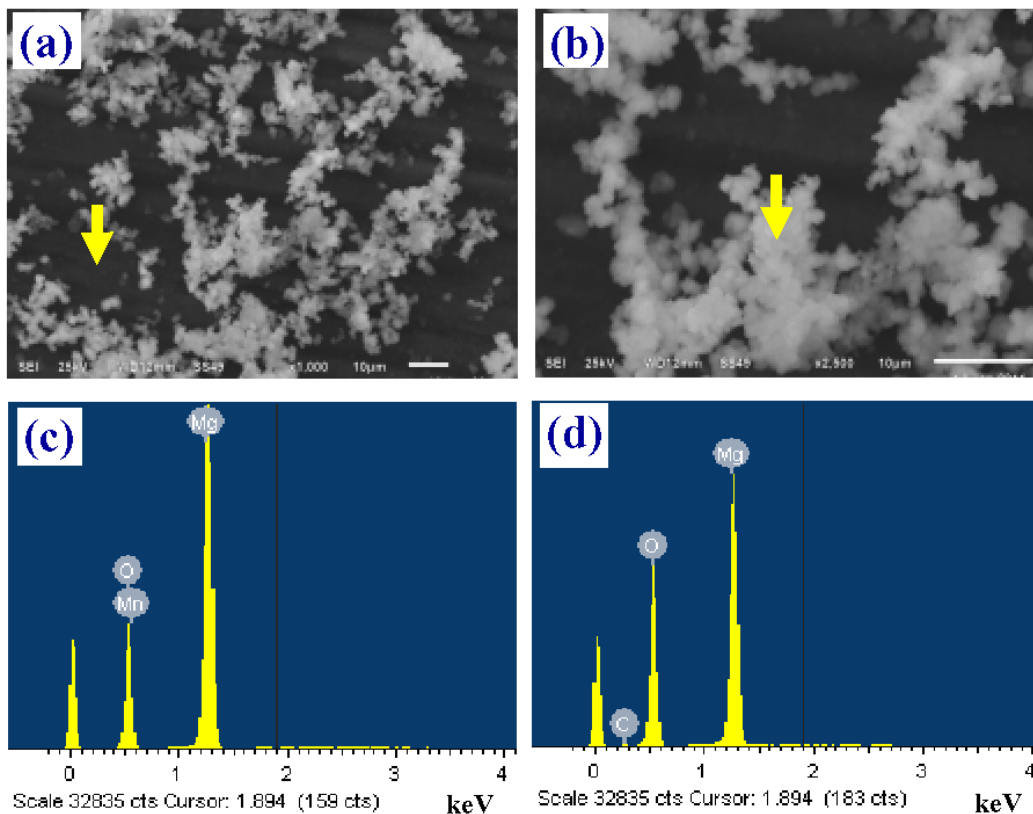


Figure 3. SEM micrographs (a) and (b) at different magnifications for magnesium surface after its immersion in 3.5% NaCl solution for 600 h; EDX profile analyses (c) and (d) taken in the selected SEM areas in image (a) and (b), respectively.

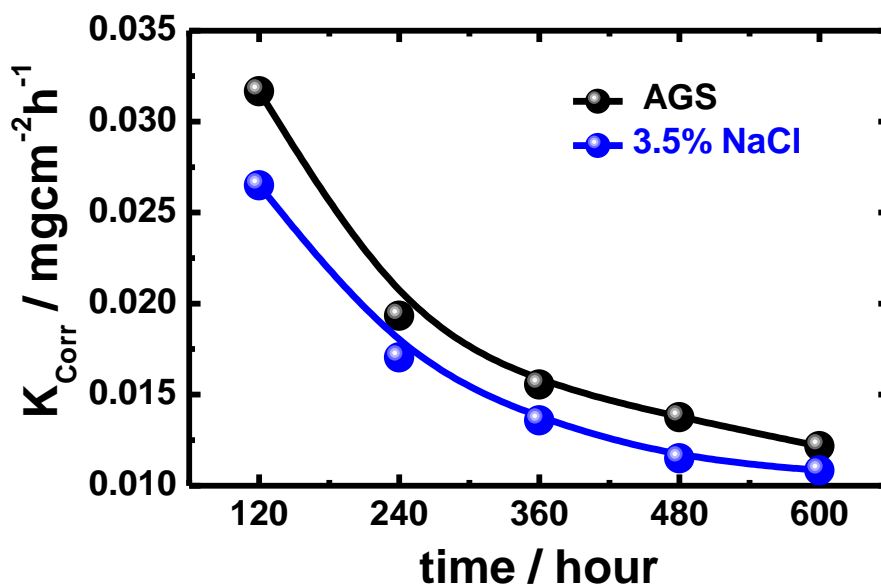


Figure 4. The change of corrosion rate (K_{Corr} / $mg\ cm^{-2}\ h^{-1}$) as a function of time for Mg coupons after its immersion in AGS and 3.5% NaCl solutions.

3.2. Cyclic potentiodynamic polarization (CPP) measurements

The potentiodynamic polarization is a powerful technique always used in determining many corrosion parameters through changing the potential values and measuring the corresponding output currents for metals and alloys in corrosive environments [46-55]. The cyclic potentiodynamic type (CPP) test in this study enabled us to record the values of corrosion potential (E_{Corr}), corrosion current density (j_{Corr}), cathodic (β_c) and anodic (β_a) Tafel slopes, pitting potential (E_{Pit}), protection potential (E_{Prot}), polarization resistance (R_P), and corrosion rate (K_{Corr}) for Mg in (a) AGS and (b) 3.5% NaCl solutions after 60 min and 6 days as respectively shown in Fig. 5. The values of β_c , E_{Corr} , j_{Corr} , β_a , E_{Prot} , R_P , and K_{Corr} were obtained from CPP curves shown in Fig. 5 according to our previous work as follows [53–55] and are presented in Table 1.

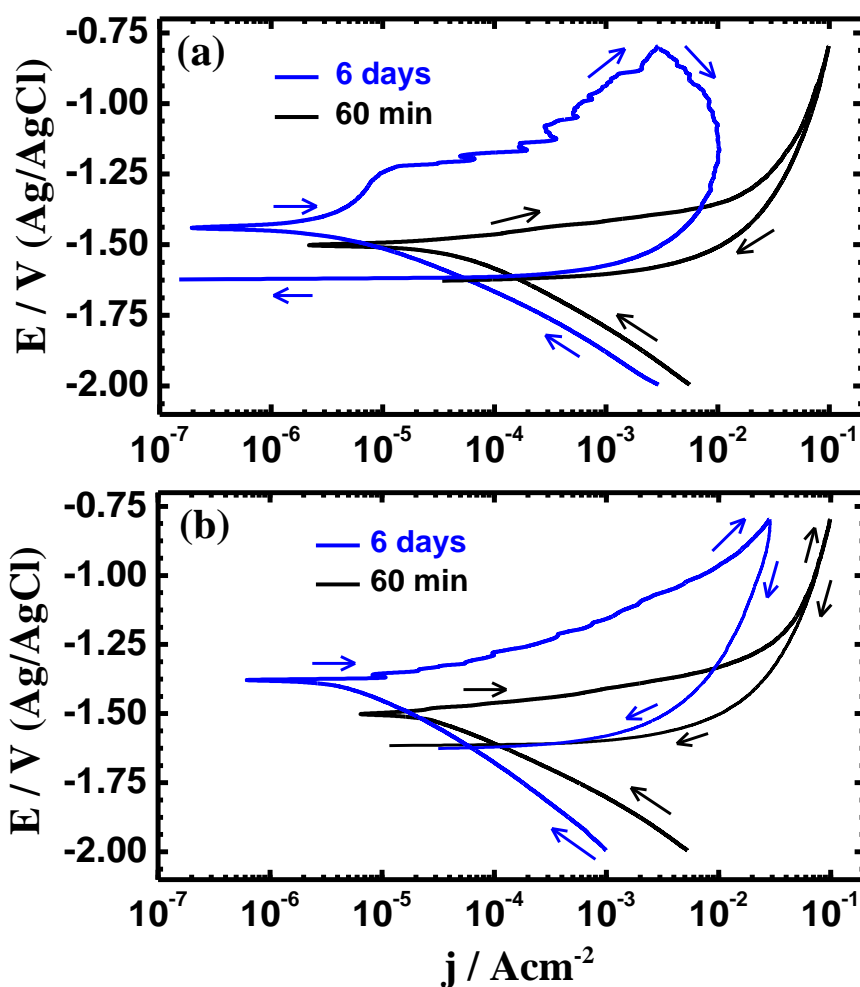


Figure 5. Cyclic potentiodynamic polarization curves for Mg electrode after its immersion in aerated (a) AGS and (b) 3.5% NaCl solutions after 60 min and 6 days, respectively.

The CPP curve recorded for Mg after its immersion in AGS for 60 min only shows that an active dissolution in the anodic branch due to the increase of potential in the positive direction as well

as the presented corrosive species in the AGS. Reversing the potential in the backward direction at the same scan rate resulted in increasing the current, which led to the appearing of a large hysteresis loop. This indicates that Mg suffered severe pitting corrosion and its protection potential is more negative than the corrosion potential as seen in Table 1. Increasing the immersion time to 6 days remarkably reduced the values of cathodic, j_{Corr} , anodic currents, and K_{Corr} , as well as increased values of R_p . This effect shifted the values of E_{Corr} and E_{Prot} to the less negative direction. This proves that increasing the immersion time of Mg in AGS before measurements highly decreases its uniform corrosion. Increasing the immersion time to 6 days also increased the area of the hysteresis loop confirming that the pitting corrosion of Mg increases with prolonging the immersion time.

Table 1. Parameters obtained from polarization curves shown in Fig. 5 for Mg electrode that was immersed in AGS and 3.5% NaCl solutions for 60 min and 6 days, respectively.

Solution	Parameter						
	$\beta_c /$ mV dec ⁻¹	$E_{\text{Corr}} /$ mV	$j_{\text{Corr}} /$ $\mu\text{A cm}^{-2}$	$\beta_a /$ mV dec ⁻¹	$E_{\text{Prot}} /$ mV	$R_p /$ $\Omega \text{ cm}^2$	$K_{\text{Corr}} /$ mmy ⁻¹
AGS after 60 min	225	-1504	51.0	65	-1620	430	1.165
AGS after 6 days	138	-1420	3.85	140	-1617	863	0.088
3.5% NaCl after 60 min	175	-1513	33.0	63	-1615	610	0.754
3.5% NaCl after 6 days	240	-1405	8.50	105	-1622	3736	0.194

The CPP curves obtained for Mg in 3.5% NaCl, Fig. 5b, after 60 min and 6 days showed almost similar behavior to that for Mg in AGS. The corrosion parameters listed in Table 1 for Mg recorded lower values of j_{Corr} and K_{Corr} and higher values of R_p . This confirms the data obtained by weight loss that both AGS and 3.5% NaCl solution cause severe corrosion for Mg and AGS is more corrosive toward Mg than 3.5% NaCl solution at the same condition. It has been reported that [56] the main corrosion product formed on the Mg surface after 10 days immersion in 3.5% NaCl is $\text{Mg}(\text{OH})_2$ according to Eq. (7). The formation of such compound on the Mg surface provides only partial protection and thus decreases the uniform corrosion of Mg in NaCl solution compared to AGS one.

3.3. Potentiostatic current–time (PCT) measurements

In order to shed more light on the dissolution of Mg and whether pitting corrosion occurs in AGS and/or 3.5% NaCl solutions at a less negative potential value, the PCT experiments were carried out. The change of the anodic currents as a function of time for Mg rod that was immersed in the aerated stagnant (a) AGS and (b) 3.5% NaCl solutions respectively for 60 min and 6 days before stepping the potential to -1200 mV vs. Ag/AgCl are shown in Fig. 6. The value of the constant potential was determined to be in the anodic branch of the polarization curves of Fig. 5. For Mg that was immersed in AGS solution for 60 min, Fig. 6a (curve 1), the initial current value recorded about 50 mAcm^{-2} ; the current then slightly increased in first 200 sec before decreasing again to reach circa 33 mAcm^{-2} . The initial current increase was due to the dissolution of an oxide film probably was

formed on the surface of the Mg during its immersion in the test solution before applying the constant potential. The decrease of current and its small fluctuations with time to the end of the experiment resulted from the dissolution of Mg to produce active site then the blocking of these sites due to the formation of corrosion products on its surface. After 6 days of Mg immersion, curve 2, the initial current recorded few microamperes then gradually increased with to reach 17.3 mAcm^{-2} by the end of the run. The higher absolute current for Mg after its immersion for 60 min than its value after 6 days indicates that Mg suffers more uniform corrosion after shorter exposure periods. The increase of current with time for Mg after its immersion in AGS for longer time suffers more pitting corrosion.

For Mg after 60 min of its immersion in 3.5% NaCl solution, Fig. 6b, curve 1, the current recorded $\sim 35 \text{ mAcm}^{-2}$ as an initial value and rapidly increased in the first few hundred seconds. The current then slightly increased and decreased accompanied by small fluctuations with a slow absolute current decrease at the end of the run. Increasing the immersion time to 6 days (Fig. 6b, curve 2) led to decreasing the initial current values to almost zero. The current then remarkably increased with time due to the occurrence of pitting corrosion.

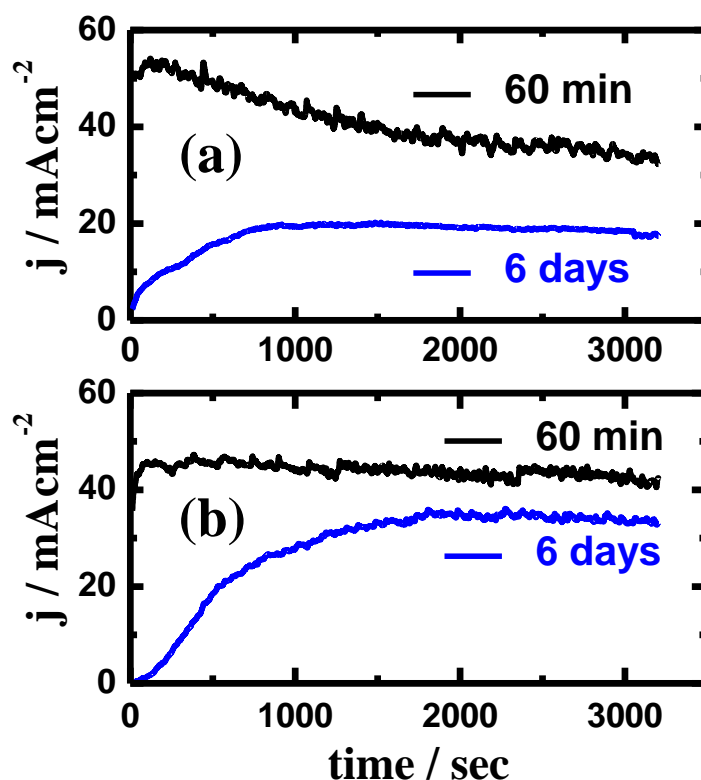


Figure 6. Potentiostatic current-time curves at -1.2 V vs. Ag/AgCl for Mg electrode after its immersion for 60 min and 6 days in aerated (a) AGS and (b) 3.5% NaCl solutions, respectively.

The initial decrease can be explained by the formation of a passive oxide film and/or corrosion products, which get thicker with time before applying the constant potential and then partially protect the Mg surface against general corrosion. This also confirms that Mg in 3.5% NaCl solutions suffers more pitting corrosion when the immersion time of Mg before measurement increases. The pitting

corrosion here occurs because pits develop at sites where, oxygen adsorbed on the Mg surface is displaced by an aggressive species such as Cl^- that is presented in the solution. This is because Cl^- has a small diameter, which allows it to penetrate through the protective oxide film and displace oxygen at the sites where metal-oxygen bond is the weakest [57]. The higher currents for Mg in AGS compared to 3.5% NaCl solution indicate that PCT data are in good agreement with the weight loss and polarization results that AGS is more corrosive towards Mg than 3.5% NaCl solution.

3.4. Electrochemical impedance spectroscopy (EIS) measurements

Fig. 7 shows the EIS Nyquist spectra that were taken at the corrosion potential of Mg after its immersion in (a) AGS and (b) 3.5% NaCl solutions, respectively for 60 minutes and 6 days. It is clearly seen from Fig. 7 that the diameter of the semicircle obtained for Mg after 60 min immersion in both AGS and NaCl solution greatly increased when the immersion time of Mg was increased to 6 days. In order to quantify the corrosion of Mg in AGS and NaCl solutions to know which is more aggressive and to also confirm the effect of prolonging the exposure time, the Nyquist plots shown in Fig. 7 were fitted to the best equivalent circuit model as shown in Fig. 8. Also, the values of the parameters obtained by fitting the equivalent circuit shown in Fig. 8 are listed in Table 2.

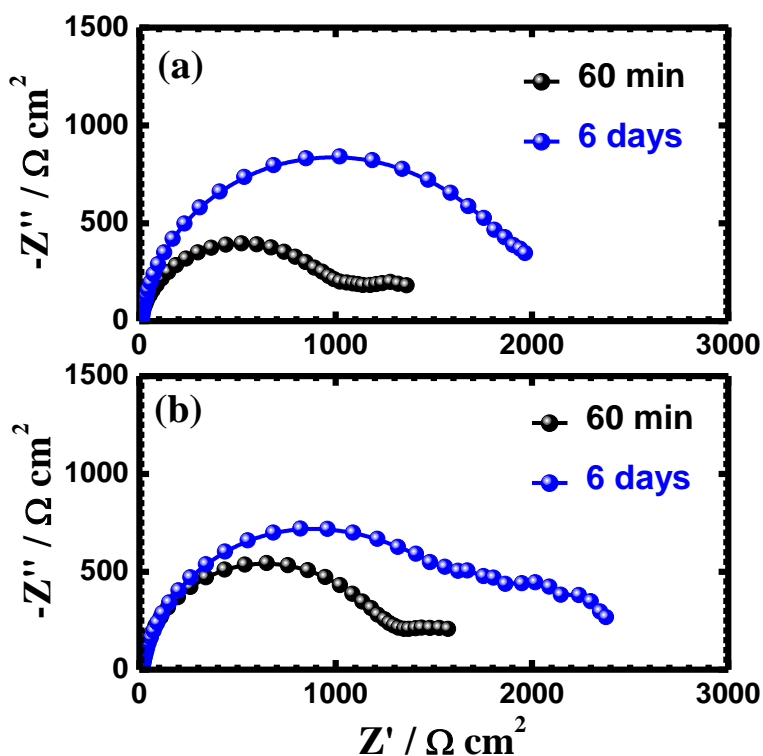


Figure 7. Nyquist plots for Mg electrode at an open-circuit potential after its immersion for 60 min and 6 days in (a) AGS and (b) 3.5% NaCl solutions, respectively.

According to usual convention, R_S represents the solution resistance between Mg and the counter (platinum) electrode, Q_1 and Q_2 the constant phase elements (CPEs), R_{P1} the resistance of a film layer formed on the surface of Mg, and R_{P2} accounts for the polarization resistance at the Mg surface. According to the previous studies [58-60], the semicircles at high frequencies in Fig. 7 are generally associated with the relaxation of electrical double layer capacitors and the diameters of the high frequency semicircles can be considered as the charge transfer resistance ($R_P = R_{P1} + R_{P2}$) [27,42]. At this condition, the value of R_P is a measure of the uniform corrosion rate as opposed to tendency towards localized corrosion.

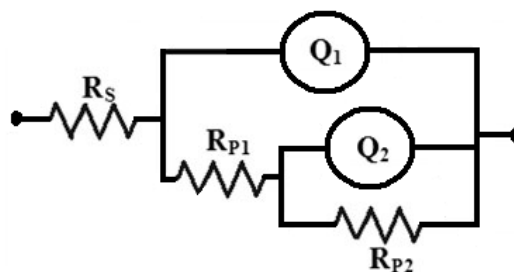


Figure 8. Equivalent circuit model used to fit the EIS Nyquist plots presented in Fig. 7.

It is seen from Table 2 that the values of R_S , R_{P1} and R_{P2} increased with increasing the immersion time of Mg from 60 min to 6 days. It is also seen that these values are higher in the NaCl solutions compared to AGS ones. The CPEs, Q_1 with its n values close to 1.0 represent double layer capacitors with some pores; the CPEs decrease, while their n -values increase with increasing the immersion time, which is expected to cover the charged surfaces and to reduce the capacitive effects. The CPEs, Q_2 with its n value close to 0.5, especially after long immersion period represent Warburg impedance and indicates that the Mg surface is more protected after 6 days exposure in the tested media and the mass transport is limited by the surface corrosion products and/or oxide film. This means that AGS is more aggressive than NaCl at this condition and confirms the weight loss, polarization and current-time data.

Table 2. EIS parameters obtained by fitting the Nyquist plots shown in Fig. 7 with the equivalent circuit shown in Fig. 8 for magnesium electrodes after 60 min and 6 days of immersion in AGS and 3.5% NaCl solutions, respectively.

Solution	Parameter						
	$R_S / \Omega\text{cm}^2$	Q_1		$R_{P1} / \Omega\text{cm}^2$	Q_2		$R_{P2} / \Omega\text{cm}^2$
		$Y_{Q1} / \mu\text{F cm}^{-2}$	n		$Y_{Q2} / \mu\text{F cm}^{-2}$	N	
AGS after 60 min	6.425	20.49	0.89	289	10.6	0.11	551
AGS after 6 days	12.07	11.06	0.91	828	1.48	0.74	942
3.5% NaCl after 60 min	8.420	0.205	0.80	320	1.058	0.11	629
3.5% NaCl after 6 days	16.36	0.153	0.89	547	0.805	0.67	884

4. CONCLUSIONS

The corrosion behavior of magnesium in Arabian Gulf seawater and 3.5% NaCl solutions after different exposure periods was reported. The study was performed using weight-loss after up to 600 hours and the surface after exposure was examined by scanning electron microscopy (SEM), and energy dispersive X-ray analyzer (EDX). The study was also complemented by cyclic potentiodynamic polarization (CPP), potentiostatic current-time (PCT) and impedance spectroscopy (EIS) measurements after 60 min and 6 days. The weight-loss data indicated that the weight-loss increases, while the corrosion rate decreases with increasing exposure time of Mg in both AGS and 3.5% NaCl solutions. The SEM micrographs and EDX profile analyses showed Mg in AGS develops shaped like mushroom in the formed corrosion products on the surface, while Mg forms oxide layer in 3.5% NaCl solutions. CPP curves proved that Mg suffers both pitting and uniform corrosion in AGS and 3.5% NaCl solutions. PCT experiments revealed that the pitting corrosion of Mg increases with increase immersion time. EIS spectra investigations confirmed that the increase of immersion time increases the surface and polarization resistances of Mg against corrosion in the tested media. The results collectively are internally consistent with each other, showing that AGS is more aggressive than 3.5% NaCl solution and the uniform corrosion decreases, while the pitting corrosion increases with increasing immersion time of Mg in both AGS and NaCl solutions from 60 min to 6 days.

ACKNOWLEDEMENT

This project was supported by King Saud University, Deanship of Scientific Research, College of Engineering Research Center.

References

1. U.C. Nwaogu, C. Blawert, N. Scharnagl, W. Dietzel, K.U. Kainer, *Corros. Sci.*, 52 (2010) 2143.
2. El-Sayed M. Sherif, A.A. Almajid, *Int. J. Electrochem. Sci.*, 6 (2011) 2131.
3. El-Sayed M. Sherif, *Int. J. Electrochem. Sci.*, 6 (2011) 5372.
4. Andrej Atrens, Nicholas Winzer, Wolfgang Dietzel, *Adv. Eng. Mater.*, 13 (2011) 11.
5. M. Hakamada, T. Furuta, Y. Chino, Y.Q. Chen, H. Kusuda, M. Mabuchi, *Energy*, 32 (2007) 1352.
6. K.U. Kainer, F. Kaiser, Eds. Magnesium alloys and technology, Weinheim Verlag GmbH & Co. KG aA Wiley-VCH GmbH (2003).
7. M.M. Avedesian, H. Baker, Eds. Magnesium and magnesium alloys, Materials Park, OH, ASM International (1999).
8. Sebastián Feliu Jr., C. Maffiotte, Alejandro Samaniego, Juan Carlos Galván, Violeta Barranco, *Electrochim. Acta*, 56 (2011) 4554.
9. A.R. Shashikala, R. Umarani, S.M. Mayanna, A.K. Sharma, *Int. J. Electrochem. Sci.*, 3 (2008) 993.
10. S.R. Agnew, "Plastic Anisotropy of Magnesium Alloy AZ31B Sheet", Magnesium Technology 2002, Ed. H. Kaplan (TMS: Warrendale, PA: 2002) 169-174.
11. G. Song, Andrej Atrens, *Adv. Eng. Mater.*, 5 (2003) 837.
12. G. Song, A. Atrens, *Advanced Engineering Materials*, 1 (1999) 11.
13. G. T. Parthiban, K. Bharanidharan, D. Dhayanand, Thirumalai Parthiban, N. Palaniswamy, V. Sivan, *Int. J. Electrochem. Sci.*, 3 (2008) 1162.
14. Guangling Song, *Advanced Engineering Materials*, 7 (2005) 563.
15. Anna Da Forno, Massimiliano Bestetti, *Advanced Research Materials*, 138 (2010) 79.

16. S. Yu. Kondrat'ev, G. Ya. Yaroslavskii, B.S. Chaikovskii, *Strength of Materials*, 18 (1986) 1325.
17. M. Carboneras, L.S. Hernandez, J.A. del Valle, M.C. Garcia-Alonso, M.L. Escudero, *J. Alloys Compd.*, 496 (2010) 442.
18. J. Kim, K.C. Wong, P.C. Wong, S.A. Kulinich, J.B. Metson, K.A.R. Mitchell, *Appl. Surf. Sci.*, 253 (2007) 4197.
19. F. Zucchi, V. Grassi, A. Frignani, C. Ponticelli, G. Trabanelli, *Surf. Coat. Technol.*, 20 (2006) 4136.
20. Saleh A. Al-Fozan, Anees U. Malik, *Desalination*, 228 (2008) 61.
21. A.M. Shams El Din, M.E. El Dahshan, A.M. Taj El Din, *Desalination*, 130 (2000) 89.
22. El-Sayed M. Sherif, A.A. Almajid, *J. Appl. Electrochem.*, 40 (2010) 1555.
23. El-Sayed M. Sherif, *J. Appl. Surf. Sci.*, 252 (2006) 8615.
24. E.M. Sherif, S.-M. Park, *J. Electrochem. Soc.*, 152 (2005) B205.
25. E.M. Sherif, S.-M. Park, *J. Electrochem. Soc.*, 152 (2005) B428.
26. E.M. Sherif, S.-M. Park, *Electrochim. Acta*, 51 (2006) 1313.
27. E.M. Sherif, S.-M. Park, *Corros. Sci.*, 48 (2006) 4065.
28. El-Sayed M. Sherif, R.M. Erasmus, J.D. Comins, *J. Colloid Interface Sci.*, 309 (2007) 470.
29. El-Sayed M. Sherif, *Mater. Chem. Phys.*, 129 (2011) 961.
30. El-Sayed M. Sherif, A.M. El Shamy, M.M. Ramla, A.O.H. El Nazhawy, *Mater. Chem. Phys.*, 102 (2007) 231.
31. A.El Warraky, H.A. El Shayeb, E.M. Sherif, *Anti-Corros. Methods Mater.*, 51 (2004) 52.
32. El-Sayed M. Sherif, R.M. Erasmus, J.D. Comins, *J. Appl. Electrochem.*, 39 (2009) 83.
33. El-Sayed M. Sherif, J.H. Potgieter, J.D. Comins, L. Cornish, P.A. Olubambi, C.N. Machio, *Corros. Sci.*, 51 (2009) 1364.
34. El-Sayed M. Sherif, R.M. Erasmus, J.D. Comins, *Electrochim. Acta*, 55 (2010) 3657.
35. El-Sayed M. Sherif, A.H. Ahmed, *Synthesis and Reactivity in Inorganic, Metal-Organic, and Nano-Metal Chemistry*, 40 (2010) 365.
36. El-Sayed M. Sherif, A.A. Almajid, F.H. Latif, H. Junaedi, *Int. J. Electrochem. Sci.*, 6 (2011) 1085.
37. El-Sayed M. Sherif, *Int. J. Electrochem. Sci.*, 6 (2011) 1479.
38. El-Sayed M. Sherif, *Int. J. Electrochem. Sci.*, 6 (2011) 3077.
39. F.H. Latief, El-Sayed M. Sherif, A.A. Almajid, H. Junaedi, *J. Anal. Appl. Pyrol.*, 92 (2011) 485.
40. El-Sayed M. Sherif, *Int. J. Electrochem. Sci.*, 7 (2012) 1482.
41. El-Sayed M. Sherif, Effects of exposure time on the anodic dissolution of Monel-400 in aerated stagnant sodium chloride solutions, *J. Solid State Electrochem.*, (2012) In Press; DOI: 10.1007/s10008-011-1438-0.
42. El-Sayed M. Sherif, J.H. Potgieter, J.D. Comins, L. Cornish, P.A. Olubambi, C.N. Machio, *J. Appl. Electrochem.*, 39 (2009) 1385.
43. El-Sayed M. Sherif, Corrosion of Duplex Stainless Steel Alloy 2209 in Acidic and Neutral Chloride Solutions and its Passivation by Ruthenium as an Alloying Element, *Int. J. Electrochem. Sci.*, 7 (2012) In Press.
44. Zhiming Shi, Andrej Atrens, *Corros. Sci.*, 53 (2011) 226.
45. S. Bender, J. Goellner, A. Heyn, E. Boese, *Mater. Corros.*, 58 (2007) 977.
46. El-Sayed M. Sherif, *J. Mater. Eng. Perform.*, 19 (2010) 873.
47. El-Sayed M. Sherif, R.M. Erasmus, J.D. Comins, *Corros. Sci.*, 50 (2008) 3439.
48. J.H. Potgieter, P.A. Olubambi, L. Cornish, C.N. Machio, El-Sayed M. Sherif, *Corros. Sci.*, 50 (2008) 2572.
49. El-Sayed M. Sherif, R.M. Erasmus, J.D. Comins, *J. Colloid Interface Sci.*, 306 (2007) 96.
50. El-Sayed M. Sherif, R.M. Erasmus, J.D. Comins, *J. Colloid Interface Sci.*, 311 (2007) 144.
51. E.M. Sherif, S.-M. Park, *Electrochim. Acta*, 51 (2006) 4665.
52. E.M. Sherif, S.-M. Park, *Electrochim. Acta*, 51 (2006) 6556.
53. Khalil A. Khalil, El-Sayed M. Sherif, A.A. Almajid, *Int. J. Electrochem. Sci.*, 6 (2011) 6184.

54. El-Sayed M. Sherif, A.A. Almajid, A.K. Bairamov, Eissa Al-Zahrani, *Int. J. Electrochem. Sci.*, 6 (2011) 5430.
55. El-Sayed M. Sherif, *Int. J. Electrochem. Sci.*, 6 (2011) 2284.
56. A.Pardo, M.C. Merino, A. E. Coy, R. Arrabal, F. Viejo, E. Matykina, *Corros. Sci.* 50 (2008) 823.
57. Z. Szklarska-Smialowska, editor. *Pitting Corrosion of Metals*, NACE International, Houston (1986).
58. El-Sayed M. Sherif, A.A. Almajid, A.K. Bairamov, Eissa Al-Zahrani, "A comparative Study on the Corrosion of Monel-400 in Aerated and Deaerated Arabian Gulf Water and 3.5% Sodium Chloride Solutions", *Int. J. Electrochem. Sci.*, 7 (2012) In Press.
59. El-Sayed M. Sherif, Ehab A. El-Danaf, Mahmoud S. Soliman, A.A. Almajid, "Corrosion Passivation in Natural Seawater of Aluminum Alloy 1050 Processed by Equal-Channel-Angular-Press", *Int. J. Electrochem. Sci.*, 7 (2012) In Press.
60. El-Sayed M. Sherif, "Corrosion Behavior of Copper in 0.50 M Hydrochloric Acid Pickling Solutions and its Inhibition by 3-Amino-1,2,4-triazole and 3-Amino-5-mercapto-1,2,4-triazole", *Int. J. Electrochem. Sci.*, 7 (2012) In Press.